Strong magnetic-field effects on the states of the helium negative ion below the He $(N=2)$ threshold

Xiaoxu Guan

Laboratory of Magnetic Resonance and Atomic and Molecular Physics, Wuhan Institute of Physics and Mathematics, The Chinese Academy of Sciences, Wuhan 430071, People's Republic of China

Baiwen Li and Lijing Wu

Chinese Center of Advanced Sciences and Technology (World Laboratory), P.O. Box 8730, Beijing, People's Republic of China and Laboratory of Magnetic Resonance and Atomic and Molecular Physics, Wuhan Institute of Physics and Mathematics, The Chinese Academy of Sciences, Wuhan 430071, People's Republic of China

(Received 10 January 2001; published 10 September 2001)

Energy levels of the $1s2l2l'\ ^2S^e$ and $^{2,4}P^{e,o}$ states of the helium negative ion in magnetic-field strengths up to 4.7011×10^4 T are calculated by using the multiconfiguration interaction approach. The extended full core plus correlation (FCPC) method and the saddle-point technique are used to construct the nonrelativistic wave functions. We have observed that the field effects on the states considered are quite unusual. In the presence of a magnetic field, three previously unobserved stable states associated with the helium $1s2p\ ^1P$ and $1s2s\ ^3S$ thresholds are predicted. The possibility of attracting an extra electron by the parent $1s^2$ state is also analyzed in the low and medium regime ($\beta\leqslant0.1$ a.u.). The opening of new decay channels of the $1s2s^2\ ^2S$ resonance state connected with the higher threshold due to field effects is analyzed. Two significantly different resonance mechanisms for the $1s2s^2$ state are proposed and discussed briefly.

DOI: 10.1103/PhysRevA.64.043402 PACS number(s): 32.60.+i, 32.10.−f, 31.10.+z, 97.10.Ex

I. INTRODUCTION

The formation of negative ions in a magnetic field has attracted considerable theoretical interest since the discovery of astrophysical compact objects with large magnetic-field strengths [1] and donor centers in semiconductors [2]. The strong magnetic field considerably compresses the atomic systems in the transverse direction. For a negative ion, the effective interaction between the internal electrons and an extra electron may be considered as an attractive one-dimensional polarization potential, which supports one bound state at least. As pointed out by Avron *et al.* [3], for example, the hydrogen negative ion has an infinite number of bound states in the presence of a magnetic field.

Very recently, advances have been made in understanding the H^- ion in magnetic fields. Al-Hujaj and Schmelcher [4] used anisotropic Gaussian-type basis sets in cylindrical coordinates to calculate the binding energies of the H^- ion in strong magnetic fields with high precision. Also, Bezchastnov *et al.* [5] presented a closed analytic expression, with a form similar to that given by Avron *et al.* [6], to estimate the binding energy of H^- in weak magnetic fields. Ho [7] investigated the combined external electric- and magnetic-field effects on the $^1S^e(1)$ and $^1D^e(1)$ Feshbach resonances of H^- below the H$(N=3)$ threshold. Compared with the H^- ion, however, the problem of a He^- ion in a strong magnetic field has received comparatively limited attention. To our knowledge, no previous works have been presented with detailed calculations for the He^- core-excited states in which two active electrons are simultaneously affected by magnetic fields. Energy levels and transition wavelengths of the He^- ion in magnetic fields are not available in the literature so far, although Avron *et al.* [6] concluded 20 years ago that He^- has at least one bound state in a strong magnetic field.

The absorption features in the observed spectra of some white dwarfs may be expected to include the so-called stationary transitions of a magnetized helium atom. Jordan *et al.* [8] presented a strong argument for the existence of atomic helium on the surface of GD229 based on the accurate wavelength spectrum obtained by Becken and Schmelcher [9]. If we assume that the atmospheres of some white dwarfs are abundant in helium atoms, we can postulate that the stable helium negative ion may also exist with a large probability even though the field-free He^- is a rather weakly bound system. The formation of He^- stable states is critically dependent upon the magnetic-field strength.

An investigation of the He^- ion will provide physical insights into the electronic properties of complex negative ions in magnetic fields. In this paper, we will investigate the $1s2l2l'\ ^2S^e$, and $^{2,4}P^{e,o}$ states of the He^- ion in magnetic fields in the energy region between the He $1s^2\ ^1S$ and $1s2p\ ^1P$ thresholds. In the energy region considered, not only bound (in the nonrelativistic limit) but also shape and Feshbach resonance states are present. It is of interest to investigate how these different states are influenced by magnetic fields. Most of the work on negative ions, such as H^-, have been concerned with the bound states induced by strong magnetic fields lying just below the ground state of the neutral atomic core. While no bound states exist for the hydrogen ion near the $2s_0$, $2p_{-1}$ and higher thresholds except for the $2p^2\ ^3P^e$ state, this is not true for the case of the He^- ion in which quadruplet states exist. In addition to the energy region below the He $1s^2$ state, we also focus our attention to the determination of possible bound states lying above the lowest Landau level of the system. In particular, the stable states induced by field effects near the helium $1s2s\ ^3S$

FIG. 1. Nonrelativistic energy of He and He$^-$ below the He$(N=2)$ threshold. The energy levels of helium are taken from Ref. [17]. The energy values of the He$^-$ $1s2s^2\,{}^2S$, $1s2s2p\,{}^4P$, $1s2s2p\,{}^2P$, and $1s2p^2\,{}^4P$ are taken from Refs. [9,10,12,13], respectively. All the energies are in hartrees.

thresholds are discussed in detail. As discussed below, our paper shows that some of the resonance states turn out to be stable states in the presence of magnetic fields. Additionally, the question whether the He$^-$ system in magnetic fields has an infinity of bound states is analyzed in general.

In the present paper, calculations of the bound or shape resonance states are based on the extended full core plus correlation method [10] while calculations of the autoionizing states are made within the multiconfiguration interaction scheme combined with the saddle-point technique [11]. Compared with field strength observed in the surface of neutron stars (10^7–10^9 T), the field strength studied here is low; on the other hand, it is supposed to be strong enough (10^4 T) to neglect the effects of spin-orbit interaction. All the discussions in this paper are limited to *the nonrelativistic approximation*. The effects of nuclear motion and relativistic autoionizing processes have not been considered in the present paper.

II. BASIC FORMULATION

A. Field-free He$^-$ ion

Before discussing the behavior of He$^-$ in magnetic fields, let us briefly overview the field-free low-lying states. Four energy levels of interest, $1s2s^2\,{}^2S$, $1s2s2p\,{}^4P$, $1s2s2p\,{}^2P$, and $1s2p^2\,{}^4P$, are shown in Fig. 1, as well as the corresponding energy levels of the helium atom [12–17]. The lowest quadruplet $1s2s2p\,{}^4P$ state lies 77.518 meV [12] below the He $1s2s\,{}^3S$. This state is not able to autoionize through the Coulomb interaction and may be considered metastable or bound in the nonrelativistic approximation. The lifetime of the $1s2s2p\,{}^4P$ state is principally dominated by the high-order relativistic autoionization process via weak spin-orbital and spin-spin interactions. The $1s2p^2\,{}^4P$ state lies 12.4 meV [16] slightly above its parent $1s2p\,{}^3P$ state and shows an apparent shape (or open channel) with a resonance character. The $1s2p^2\,{}^4P$ state of He$^-$ ion is different from those of other neutral (or positive) three-electron systems in that the state in lithium lies below the $1s2p\,{}^3P$ threshold and is a metastable rather than a potential shape resonance. Other states, $1s2s^2\,{}^2S$ and $1s2s2p\,{}^2P$, lie, respectively, below the corresponding parent states $1s2s\,{}^3S$ and $1s2s\,{}^1S$, and show the significant Feshbach (or closed channel) resonances. The autoionizing channel $1s^2\epsilon s\,{}^2S$ and $1s^2\epsilon p\,{}^2P$ are, respectively, open for these two states. It should be emphasized that although the $1s2s2p\,{}^2P$ state lies above the He $1s2s\,{}^3S$ state, it cannot be designated to be a ${}^2P$ shape resonance (see Ref. [14] for further details and references therein). In fact, the $1s2s2p\,{}^2P$ state is a broad Feshbach resonance formed by the dipole mixing of the $[(1s2s)^1S,2p]$ and $[(1s2p)^1P,3d]$ configurations.

B. Hamiltonian and symmetries

We assume that the magnetic field is pointing towards the positive z direction and we assume also that the nuclear mass is infinite. The nonrelativistic Hamiltonian of the three-electron He$^-$ in a homogeneous magnetic field can be expressed in spherical coordinates as

$$H=\sum_{i=1}^{3}\left(-\frac{1}{2}\nabla_i^2-\frac{2}{r_i}\right)+\frac{1}{2}\sum_{i\neq j=1}^{3}\frac{1}{r_{ij}}+\sum_{i=1}^{3}\left[\frac{1}{3}\beta^2r_i^2-\frac{2}{3}\sqrt{\frac{\pi}{5}}\beta^2r_i^2Y_{20}(\theta_i,\phi_i)\right]+\beta(L_z+2S_z), \tag{1}$$

where the field parameter β is given by $\beta=B/B_0$, with $B_0=4.7011\times10^5$ T. The r_i represent the distances between the electrons and the nucleus; the r_{ij} the distances between electrons; and the $Y_{lm}(\theta,\phi)$ are the usual spherical harmonics. Because of the external strong magnetic field acting on the electrons, the spherical symmetry of the field-free system is broken, and then the total angular momentum quantum numbers L are not good quantum numbers any longer. In the presence of the external magnetic field, the total spin angular momentum S, the total azimuthal quantum numbers M_L and M_S, and the total z-parity $\Pi_z=(-1)^{\Sigma_{i=1}^{3}(l_i-m_i)}$ are good quantum numbers and may be used to denote the states. Since our paper is concerned with relatively low-field-strength regions ($\beta<1$), in addition to the conserved quantum numbers, we use field-free notation to approximately describe the He$^-$ ion. With this notation, one can easily follow how a particular state evolves with increasing field strength. For simplicity, we omitted the total spin magnetic quantum number M_S in the notation of states since only states with $M_S=-S$ are discussed throughout this paper.

C. Construction of the configuration interaction wave functions

We are interested both in bound and autoionizing states. Different treatments are necessary for these two kinds of states. Special attention should be paid to the autoionizing $1s2s^2\,{}^2S$ and $1s2s2p\,{}^2P$ states. In this paper, the bound and potential shape resonance states are treated by using the Rayleigh-Ritz variational method, and the saddle-point technique has been applied to describe the autoionzing states of He^- in magnetic fields. For the configurations $1s2l2l'$ studied here, the inner $1s$ electron is tightly bounded, but the two outer active electrons are more sensitive to the external fields. Even relatively low-field strengths ($\beta<1$) have a significant influence on the electronic motion. Considering the fact that the He^- ion is a three-electron system with a quite weak binding, we restrict ourselves to investigate the structure properties of He^- in the low-field region ($\beta\leqslant 0.2$ a.u.), which is characteristic of the field strengths found in white dwarfs.

1. Wave functions of the bound and shape resonance states

Based on the considerations above, the wave functions are expressed in terms of spherically symmetric basis sets, i.e., Slater-type orbitals. For the bound and shape resonance states the wave function of the system takes the form [10]

$$\Psi(1,2,3)=A\left[\sum_i C_i\Phi_i(1,2)\psi_i(3)+\sum_i C_i\Phi_i(1,2,3)\right]. \tag{2}$$

The summation in the first term on the right-hand side of Eq. (2) is over all possible $core+l$ configurations. At first glance, of course, it seems that there does not exist a meaningful two-electron core for the $1s2p^2\,{}^4P$ and $1s2s2p\,{}^4P$, since only one electron occupies the inner $1s_0$ orbital. Notice, however, that the doubly excited states in the presence of magnetic fields are different from those in the field-free case. Consider the $1s2p^2\,{}^4P$ state as an example to illustrate this point. Although the angular momentum of a single electron is not a conserved quantum number, the z component of the total angular momentum, with eigenvalue $M_L=\Sigma_i m_{li}=-1$, is conserved. Thus, a number of possible angular configurations with $(m_1,m_2,m_3)=(0,0,-1)$, $(0,1,-2)$, and $(1,-1,-1)$, . . . , should be incorporated into the total wave function, in order to take account of the angular correlations. It may be expected that the contribution to the energy from the $(m_1,m_2,m_3)=(0,0,-1)$ configuration is dominant compared with the other ones. Combined with the conserved z component of parity, we can reasonably denote the state as $1s_02p_02p_{-1}\,{}^4P_{-1}$. It is well known that in the case of hydrogen, the $2p_{-1}$ electron shows a different character than the $2p_0$ electron: the $2p_{-1}$ electron is more tightly bounded in a magnetic field [1]. In other words, the $2p_{-1}$ and $2p_0$ electrons play quite different roles (which may be also seen from the calculations that follow) in determining the electronic properties of the $1s2p^2\,{}^4P_{-1}$ state. As a result, we may take He $1s2p_{-1}$ as our first two-electron core and He $1s2p_0$ as the second one, both of which are paired with the $2p_0$ and $2p_{-1}$ electrons, respectively, to build up the total wave function.

In Eq. (2), $\Phi_i(1,2)$ and $\psi_i(3)$ are expressed as linear combinations of Slater-type orbitals, i.e.,

$$\Phi_i(1,2)=A\sum_{i,k,n} C_i\langle l_1m_1l_2m_2|l_{12}m_{12}\rangle r_1^k r_2^n \times\exp(-\alpha_{l_1}r_1-\beta_{l_2}r_2)Y_{l_1m_1}(\Omega_1) \times Y_{l_2m_2}(\Omega_2)\chi(1,2) \tag{3}$$

and

$$\psi_i(3)=\sum_n d_n r_3^n e^{-\beta r_3}Y_{l_3m_3}(\Omega_3)\chi(3). \tag{4}$$

In the actual calculations, the wave function of each atomic core [see Eq. (3)] was predetermined and was treated as a single term in the wave function of the three-electron system.

Correlation effects are not negligible for doubly excited states in magnetic fields. The last term of Eq. (2), necessary for accurate calculations, is constructed in terms of Slater-type orbitals. This contribution is designed to describe the correlation between three electrons, such as the core-polarization effect induced by the outer electron. The strategy used in this work has a substantial advantage over other CI approaches in that the size of the generalized eigenvalue problem is considerably reduced given that the wave function of each core state consists of a single term. For instance, the dimension of the eigenvalue problem needed to be solved does not exceed 500 basis functions in most cases, thus, avoiding the problems due to numerical instabilities. These considerations apply as well to the case of the $1s2s_02p_{-1}\,{}^4P_{-1}$ state.

2. Wave functions of autoionizing states

We will use the saddle-point technique [11] to build the wave function for autoionizing states in strong magnetic fields. The lifetimes of the $1s2s^2\,{}^2S_0$ and $1s2s2p\,{}^2P_{-1}$ resonances of interest, strongly depend on the nonrelativistic autoionzing process via the direct Coulomb interaction since both states have a $1s_0$ vacancy orbital. Similarly to the occupied orbitals, the vacancy orbital is also influenced by the external magnetic field, thus, this single-electron orbital is also constructed using a linear combination of spherical Slater-type basis sets. The closed-channel wave function of the resonance state is given by

$$\Psi(1,2,3)=A\sum_i C_i[1-P(i)]\Phi_i(1,2,3), \tag{5}$$

where $P(i)=|\psi_{1s_0}(i)\rangle\langle\psi_{1s_0}(i)|$ is a projection operator. $\Phi_i(1,2,3)$ is similar to the second term of Eq. (2), which has been constructed in terms of Slater-type orbitals. In order to span as well as possible the function space with broken

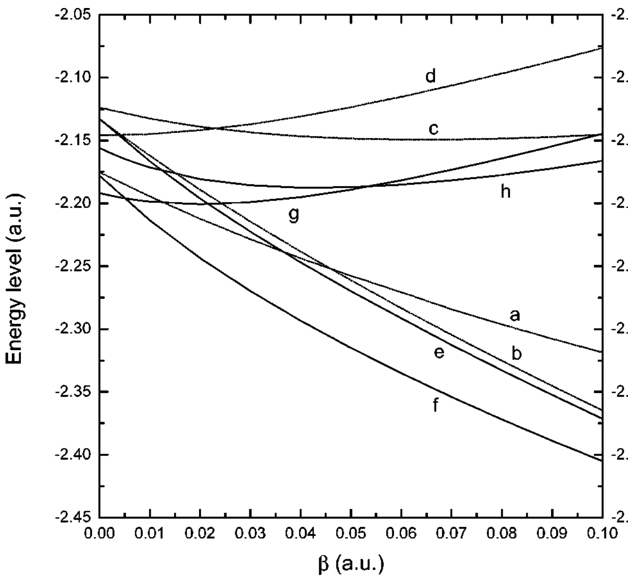

FIG. 2. Energy levels of He $1s2s\,{}^3S_0(a)$, $1s2p_{-1}\,{}^3P_{-1}(b)$, $1s2p_{-1}\,{}^1P_{-1}(c)$, and $1s2s\,{}^1S_0(d)$ states and He^- $1s2p_02p_{-1}\,{}^4P_{-1}(e)$, $1s2s_02p_{-1}\,{}^4P_{-1}(f)$, $1s2s_0^2\,{}^2S_0(g)$, and $1s2s_02p_{-1}\,{}^2P_{-1}(h)$ states in magnetic fields up to $\beta=0.10$ a.u. ($\beta=B/4.7011\times10^5$ T). All the energies are in hartrees.

spherical symmetry, it should be emphasized that not only occupied but also unoccupied (vacancy) electron orbitals contain nonlinear exponent parameters. The optimal variational energy of the resonance state, $E=\langle\Psi|H|\Psi\rangle/\langle\Psi|\Psi\rangle$, is determined by a process of minimization and maximization with respect to the nonlinear parameters of the occupied and unoccupied orbitals, respectively.

III. RESULTS AND DISCUSSION

Figure 2 shows the energy levels of the He^- states studied, as well as the corresponding parent He states as continuous functions of the field strength up to 4.7011×10^4 T. Numerical results for the energy levels of the He^- ion are listed in Table I.

A. Bound and shape resonance states in magnetic fields

Given that spherically symmetric basis sets are used to construct the wave function in which a number of angular-spin components is included, it is important to examine the convergence of the energy eigenvalues as the number of components is increased. As a typical example, the energy convergence of the $1s2p_02p_{-1}$ state at $\beta=0.10$ a.u. is given in Table II. The helium atom orbitals $1s2p_{-1}$ and $1s2p_0$ in the presence of the magnetic field are regarded as two core states in Eq. (2). Accurate energies of helium obtained with Hylleraas-type wave functions are also listed for comparison [18]. It is interesting to observe that the two $core+l$ configurations, $[1s2p_{-1}+l]$ and $[1s2p_0+l]$, show quite different convergence patterns. The contribution to the energy from the $[1s2p_{-1}+l]$ component is obviously larger than that of the $[1s2p_0+l]$ component for the same of l. Figure 3 shows the convergence with l at $\beta=0.10$ a.u. As one can see, the convergence of the $[1s2p_{-1}+l]$ components is slower. With the help of a single-particle picture, this can be explained as follows: the nodal surfaces of the $2p_0$ and $2p_{-1}$ states are, respectively, transverse and parallel to the direction of the magnetic field. In the presence of a magnetic field, the $2p_{-1}$ electron is squeezed in a smaller region along the z axis compared with the $2p_0$ electron, whose charge density takes nonzero values along the z axis. As a result, the $2p_0$ electron has a more pronounced cylindrical symmetry at a specified field strength. Thus, it is not surprising then that the $[1s2p_{-1}+l]$ components show a relatively slow convergence rate given that we are using basis sets with spherical symmetry to describe these states. From Table II, we see also that the contribution from the [(2,2)1,0] component is the largest among the three-electron correlation terms. This sug-

TABLE I. Energy of the He^- $1s2l2l'\,{}^2S^e$ and ${}^{2,4}P^{e,o}$ states in the field regime $\beta\leqslant0.10$ a.u. All the energies are in hartrees.

β(a.u.)	$1s2s^2\,{}^2S_0$	$1s2s_02p_{-1}\,{}^2P_{-1}$	$1s2s_02p_{-1}\,{}^4P_{-1}$	$1s2p_02p_{-1}\,{}^4P_{-1}$
0.000	−2.191 772	−2.155 752	−2.178 017	−2.132 637
0.002	−2.193 633	−2.159 565	−2.185 815	
0.004	−2.195 252	−2.163 018		
0.006	−2.196 635	−2.166 134		
0.008	−2.197 793			
0.010	−2.198 712	−2.171 476	−2.213 567	−2.166 559
0.020	−2.200 521	−2.180 716	−2.243 481	−2.196 144
0.030	−2.199 043	−2.185 627	−2.269 752	−2.222 563
0.040	−2.194 989	−2.187 542	−2.293 392	−2.246 969
0.050	−2.189 013	−2.187 183	−2.315 028	−2.269 831
0.060	−2.181 659	−2.185 113	−2.335 132	−2.291 835
0.070	−2.173 304	−2.181 635	−2.353 990	−2.312 767
0.080	−2.164 233	−2.177 470	−2.371 833	−2.332 960
0.090	−2.154 624	−2.172 150	−2.388 840	−2.352 444
0.100	−2.144 594	−2.166 093	−2.404 995	−2.371 360

TABLE II. Energy convergence of the He $1s2p_{-1}\ ^3P_{-1}$ and $1s2p_0\ ^3P_0$ cores and the He$^-$ ion $1s2p_02p_{-1}\ ^4P_{-1}$ at $\beta=0.10$ a.u. *Core*1 and $core2$ represent the first ($1s2p_{-1}\ ^3P_{-1}$) and second ($1s2p_0\ ^3P_0$) atomic cores, respectively. N is the number of terms included in the angular component. All the energies are in hartrees.

$1s2p_{-1}\ ^3P_{-1}$ $(l_1,l_2)l_{12}$	N	$-\Delta E$	$1s2p_0\ ^3P_0$ $(l_1,l_2)l_{12}$	N	$-\Delta E$	$1s2p_02p_{-1}\ ^4P_{-1}$ $[(l_1,l_2)l_{12},l_3]L$	N	$-\Delta E$
(0,1)1	35	2.362 039 9	(0,1)1	35	2.290 947 7	$[core1,1]1$	11	2.342 284 3
(1,2)1	24	0.001 260 3	(1,2)1	24	0.001 097 9	$[core2,1]1$	11	0.005 808 9
(2,3)1	15	0.000 072 0	(2,3)1	15	0.000 059 7	$[core1,3]3$	9	0.011 783 5
(3,4)1	19	0.000 010 8	(3,4)1	19	0.000 008 9	$[core2,3]3$	9	0.001 925 2
(4,5)1	10	0.000 002 3	(4,5)1	10	0.000 001 9	$[core1,5]5$	7	0.003 025 7
(5,6)1	6	0.000 000 6	(5,6)1	6	0.000 000 5	$[core2,5]5$	7	0.000 142 3
(6,7)1	3	0.000 000 2	(6,7)1	3	0.000 000 1	$[core1,7]7$	5	0.001 153 0
(0,3)3	16	0.001 263 8	(0,3)3	16	0.002 931 3	$[core2,7]7$	5	0.000 014 1
(0,5)5	19	0.000 035 5	(1,2)3	19	0.000 002 4	$[core1,9]9$	3	0.000 514 4
Total	147	2.364 685 5	(0,5)5	15	0.000 136 8	$[core2,9]9$	3	0.000 001 8
		2.364 69[a]	(0,7)7	15	0.000 008 0	$[core1,11]11$	3	0.000 252 0
			Total	177	2.295 195 3	$[core2,11]11$	3	0.000 000 3
					2.295 21[a]	[(1,1)1,0]1	63	0.000 451 2
						[(2,2)1,0]1	43	0.003 365 6
						[(3,3)1,0]1	15	0.000 225 3
						[(1,1)1,2]1	21	0.000 005 8
						[(1,1)2,2]1	31	0.000 004 7
						[(1,0)1,1]1	20	0.000 001 5
						[(4,4)1,0]1	22	0.000 025 5
						[(5,5)1,0]1	13	0.000 007 0
						[(1,2)1,1]1	10	0.000 003 4
						[(1,2)2,1]1	10	0.000 000 2
						[(1,1)2,0]2	34	0.000 007 5
						[(2,2)0,0]3	22	0.000 107 3
						[(3,3)3,0]3	15	0.000 249 4
						[(5,5)5,0]5	15	0.000 000 3
						Total	410	2.371 360 1

[a]Scrinzi [18].

gests that there exist a strong coupling between the $1s2p^2\ ^4P_{-1}$ and $1s3d^2\ ^4P_{-1}$ configurations.

For the field-free case, the $1s2p^2\ ^4P_{-1}$ state is a potential shape resonance state. We have found, however, an interesting and surprising result: as can be seen from Fig. 2, the $1s2p^2\ ^4P_{-1}$ state turns out to be a bound state at field strengths $\beta \geqslant 0.002$ a.u. In Table III, we show the total-energy and electron-detachment-energy values of the bound states induced by field effects. The ionization threshold in the magnetic field is expressed as

$$E_T=\beta(|M_L|+M_L+2M_S+3)-\mathcal{E}_B(\text{He},1snl\ ^3l), \quad (6)$$

where $\mathcal{E}_B(\text{He},1snl\ ^3l)$ represents the (binding) energy required to completely dissociate the helium atom into two free electrons and a nucleus. It reads

$$\mathcal{E}_B(\text{He},1snl\ ^3l)=\beta(|M_{L_{12}}|+M_{L_{12}}+2M_{S_{12}}+2)-E_{tot}(\text{He}). \quad (7)$$

In our present case, M_L, $M_{L_{12}}\leqslant 0$, $M_S=-3/2$, and $M_{S_{12}}=-1$, thus $E_T=-\mathcal{E}_B(\text{He},1snl\ ^3l)$. With Eqs. (6) and (7), the electron detachment (or binding) energy reads

$$I(\text{He}^-)=E_T-E_{tot}(\text{He}^-)=E_{tot}(\text{He})-E_{tot}(\text{He}^-), \quad (8)$$

where $E_{tot}(\text{He})$ and $E_{tot}(\text{He}^-)$ are the total energies in the magnetic field of He and He$^-$, respectively.

In the case of the $1s2s_02p_{-1}\ ^4P_{-1}$ state, we find that its energy is always lower than the energy of the He $1s2s\ ^3S$ threshold, as the field strength is increased. Similar to the field-free case, we can consider the $1s2s_02p_{-1}\ ^4P_{-1}$ as a bound state if we neglected the relativistic spin-induced autoionizing process. The binding energy of this state increases when the field strength is increased. A natural question can then be raised: does the series $1s2s_onp_{-1}\ ^4P_{-1}$ exist below the He $1s2s\ ^3S_0$ threshold? To answer this question, we have calculated the $1s2s_0np_{-1}\ ^4P_{-1}$ states in a magnetic field, as shown in Fig. 4. In the absence of a field, only the $1s2s2p\ ^4P_{-1}$ state lies below the helium $1s2s\ ^3S$ state. But we found that the $1s2s3p\ ^4P_{-1}$ will become a bound state after the field strength increases beyond 0.08 a.u.; other $1s2snp\ ^4P-1$ states still remain as resonances. In other words, only a *finite* number of bound states with a given symmetry exist near the $1s2s\ ^3S$ threshold. Notice that this does not contradict the universal premise that states that an

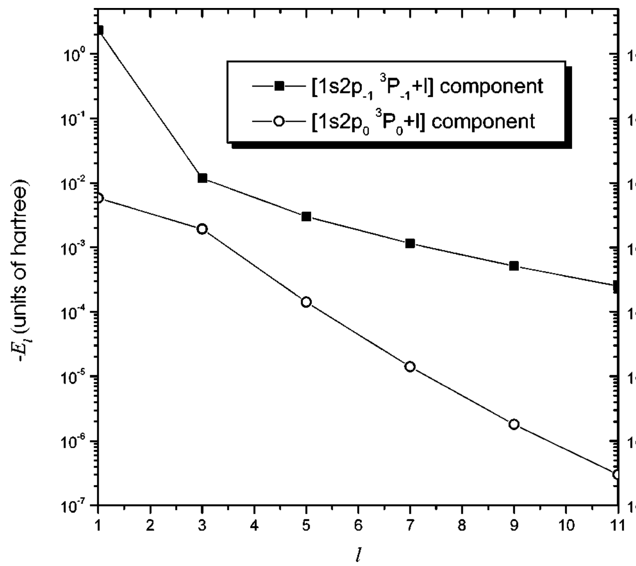

FIG. 3. Energy convergence of the He^- $1s2p_02p_{-1}\,{}^4P_{-1}$ state with increasing angular momentum. $-E_l$ is the contribution to energy from the $[1s2p_0+l]$ or $[1s2p_{-1}+l]$ component. Field strength is $\beta=0.10$ a.u. $=4.7011\times10^4$ T. All the energies are in hartrees.

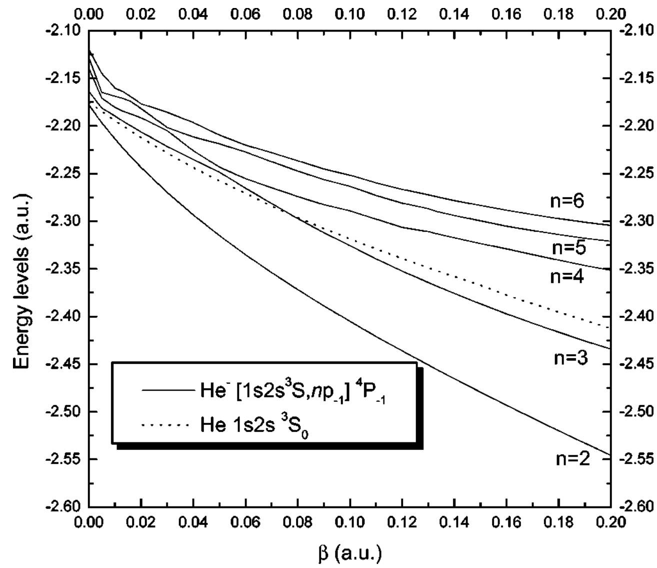

FIG. 4. Energy levels of the He $1s2s_0\,{}^3S_0$ and He^- $1s2s_0np_{-1}\,{}^4P_{-1}$ states in magnetic fields up to $\beta=0.20$ a.u. ($\beta=B/4.7011\times10^5$ T). The $1s2s_03p_{-1}\,{}^4P_{-1}$ state will become a bound state lying below the He $1s2s\,{}^3S_0$ threshold, while the field strength exceeds 0.08 a.u. All the energies are in hartrees.

infinite number of bound states exist for negative ion systems in magnetic fields, since new bound states may be expected to exist below other ionization thresholds. A reason for the appearance of new bound states at large enough field strengths is that the anticrossing between the second- and the third-energy levels occurs around $\beta\simeq0.05$ a.u. due to the identical symmetry of the configurations. As a result, the energy of the second eigenstate decreases further, and eventually lies below the helium $1s2s\,{}^3S$ threshold.

To check whether the bound states induced by the magnetic field occur only in negative ion systems, it is useful to compare the helium negative ion with the neutral lithium atom. The *field-free* lithium Rydberg series $1s2snp\,{}^4P(n=2,3,4,\ldots)$ converges, with increasing n, to the parent

TABLE III. Total energy (E_{tot}) and electron detachment energy (I) of the bound states induced by magnetic fields. All the energies are in hartrees.

	$1s2p_02p_{-1}\,{}^4P_{-1}$		$1s2s_03p_{-1}\,{}^4P_{-1}$		$1s2s_03d_{-2}\,{}^4D_{-2}$	
β (a.u.)	E_{tot}	I	E_{tot}	I	E_{tot}	I
0.002	−2.139 504	0.000 40				
0.005	−2.150 392	0.002 51			−2.185 216	0.000 18
0.01	−2.166 559	0.004 45			−2.195 595	0.001 13
0.02	−2.196 144	0.007 03			−2.216 075	0.003 85
0.03	−2.222 563	0.008 12			−2.235 312	0.006 72
0.04	−2.246 969	0.008 59			−2.253 127	0.009 43
0.05	−2.269 831	0.008 66			−2.269 616	0.011 93
0.06	−2.291 835	0.008 43			−2.284 912	0.014 26
0.07	−2.312 767	0.008 14			−2.300 326	0.016 06
0.08	−2.332 960	0.007 77	−2.297 192	0.000 94	−2.314 256	0.018 00
0.09	−2.352 444	0.007 25	−2.312 089	0.004 42	−2.327 467	0.019 80
0.10	−2.371 360	0.006 68	−2.325 692	0.007 12	−2.340 091	0.021 52
0.11			−2.339 540	0.010 51	−2.351 577	0.022 54
0.12			−2.352 260	0.013 17	−2.363 117	0.024 03
0.14			−2.375 843	0.017 69	−2.385 009	0.026 86
0.15			−2.386 773	0.019 56	−2.396 476	0.029 27
0.16			−2.397 217	0.019 63	−2.410 210	0.032 63
0.19			−2.425 646	0.021 60	−2.437 271	0.033 22
0.20			−2.434 255	0.021 66	−2.446 613	0.034 02

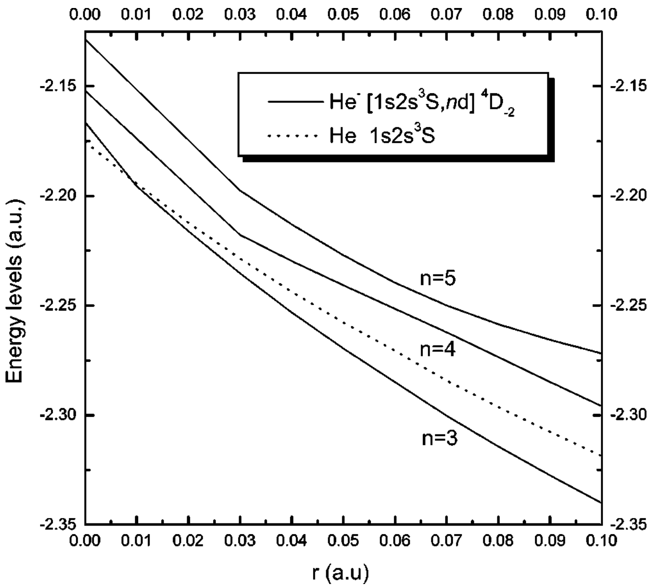

FIG. 5. Energy levels of the He $1s2s_0\,{}^3S_0$ and He$^-$ $1s2s_0nd_{-2}\,{}^4D_{-2}$ states in magnetic fields up to $\beta=0.10$ a.u. ($\beta=B/4.7011\times10^5$ T). The $1s2s_03d_{-2}\,{}^4D_{-2}$ state will become a bound state lying below the He $1s2s\,{}^3S_0$ threshold, while the field strength exceeds 0.005 a.u.

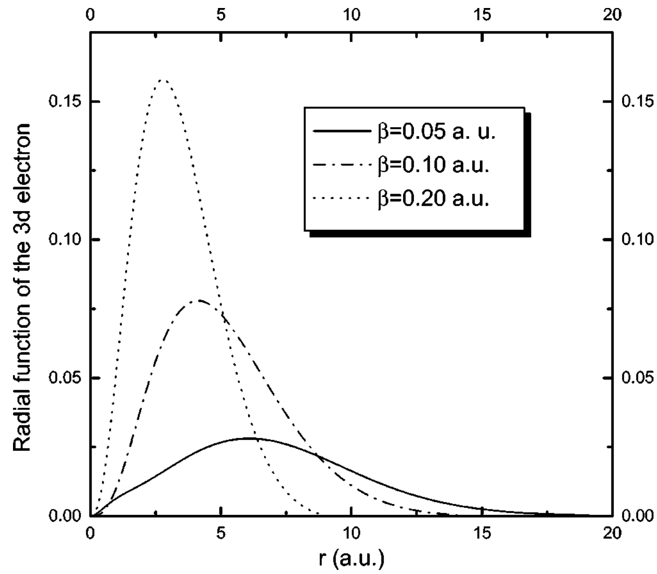

FIG. 6. The non-normalized radial function of the $3d$ electron in the He$^-$ $1s2s_03d_{-2}\,{}^4D_{-2}$ state. The field strengths are 0.05, 0.10, and 0.20 a.u. (1 a.u.$=4.7011\times10^5$ T), respectively.

$1s2s\,{}^3S$ state. In our calculations, the magnetic field does not produce any new stable states in lithium below the Li$^+1s2s\,{}^3S$ threshold. All of the $1s2snp\,{}^4P(n=2,3,4,\ldots)$ states in a magnetic field are always lower than the $1s2s\,{}^3S$ state. We concluded then that the appearance of new bound states induced by an external magnetic field is merely a characteristic of negative ions. We emphasized that in Li, Rydberg series do exist due to the long-range Coulomb interaction between an external electron and the Li$^+$ core.

In addition to the ${}^4P^e_{-1}$ states, a new stable ${}^4D^e_{-2}$ state is also found near the $1s2s\,{}^3S$ threshold, as one can see from Fig. 5. In order to obtain a better insight into the bound ${}^4D^e_{-2}$ state induced by field effects, we have used a parentage projection method to classify the state structure. First, the two-electron parent $(1s2s)\,{}^3S$ wave function in magnetic fields may be easily determined. The non-normalized radial function of the extra electron is thus expressed by [19]

$$f(r_3)=\sum_{m_{12},m_3,m_{s_{12}},m_{s_3}} C\Phi^{m_{12},m_{s_{12}}}_{1s1s}(1,2)Y_{l_3,m_3}(\Omega_3)\times\chi_{s_3,m_{s_3}}(3)|\Psi(1,2,3)\rangle, \tag{9}$$

where $l_3=2$ and $s_3=1/2$ for the ${}^4D$ symmetry. C is the product of Clebsch-Gordan coefficients

$$C=\langle l_{12}m_{12},l_3m_3|LM_L\rangle\langle S_{12}m_{s12},s_3m_{s3}|SM_S\rangle. \tag{10}$$

The integration in Eq. (9) is made over all the spatial and spin coordinates except the radial coordinate r_3.

For the He$^-$ $[(1s2s)^3S,nd]\ {}^4D_{-2}$ state with lowest energy, the radial functions $f(r_3)$ are plotted in Fig. 6 at three field strengths ($\beta=0.05$, 0.10, and 0.20 a.u.). It can be seen that the radial functions with d symmetry have no nodes. This indicates that we can reasonably identify such state by $[(1s2s)^3S,3d]^4D_{-2}$, which turns out to be a bound state as the field strength exceeds about 0.005 a.u. The detachment energies for this state are also listed in Table III. From Fig. 6, as we expected, the density distribution for the $3d$ electron concentrates in a smaller region near nucleus as the field strength is increased.

Next, we discuss the possible existence of bound states below the He $1s^2\,{}^2S$ threshold in magnetic fields. If there exist bound states below the $1s^2$ threshold, we may approximately designate them as $1s^2nl$. In this paper, we study the possible existence of a bound state near the He $1s^2$ state by varying the nonlinear parameter in the outer electron orbital in order to change both the energy and the space distribution of the state of interest [20]. The latter one is roughly measured by the average radius $R=\langle\Psi|\Sigma^3_{i=1}r_i|\Psi\rangle$. If a state contains bound state components, the energy, as a continuous function of R, will show a minimum at a specified R value. We take the $1s2s^2\,{}^2S_0$ state at $\beta=0.01$ a.u. for example, to illustrate this point (see Fig. 7). At $\beta=0.01$ a.u. the dependence of the energy of the $1s^22s\,{}^2S$ *pseudo* state on the R is shown in Fig. 8. Given the slow convergence, the energy calculation included three angular components: core+0, core+2, and core+4. We can see that the energy is monotonically decreasing when R is increased. This preliminary test shows that in the region $\beta<0.1$ a.u. no stable or bound states are found for the symmetry of interest. Even though there exist bound states with zero angular momentum of the extra electron, the binding energies are expected to be much smaller than those of the H$^-$ ion, due to the smaller polarizability of the helium $1s^2$ configuration. Thus, a more sophisticated approach, in which the external electron is described in cylindrical coordinates, has to be used to make a definitive statement. This will be done in future work.

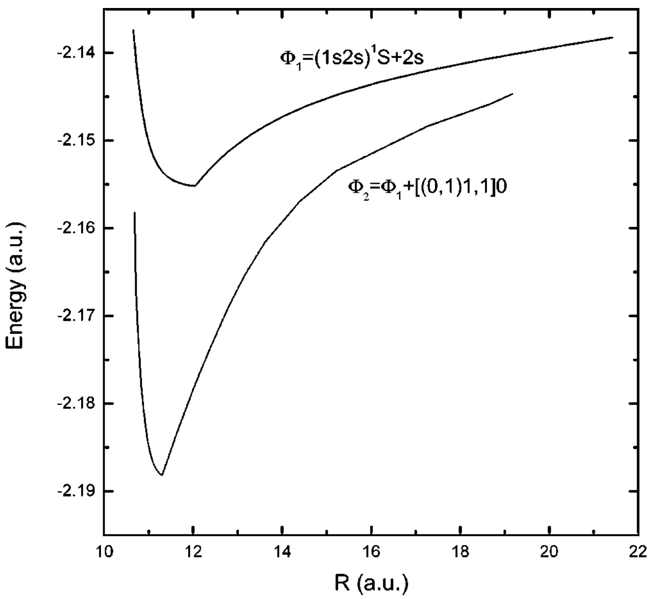

FIG. 7. Energy of He^- $1s2s^2\,{}^2S_0$ vs R ($\langle\Psi|\Sigma_{i=1}^3 r_i|\Psi\rangle$) at $\beta=0.01$ a.u. ($\beta=B/4.7011\times10^5$ T). Φ_1 represents that only the $(1s2s)^1S+2s$ configuration is included in the wave function. Φ_2 represents that not only the $(1s2s)^1S+2s$ but also the $[(0,1)1,1]0$ configuration are included. A stationary point around $R=11.3$ a.u. may be observed.

B. Autoionizing resonance states: $1s2s^2\,{}^2S_0$ and $1s2s2p\,{}^2P_{-1}$

The energies of the autoionizing states calculated in this paper are obtained using multiconfiguration wave functions combined with the saddle-point technique.

For the $1s2s^2\,{}^2S$ state at the $\beta=0.01$ a.u. convergence as a function of increasing angular-spin components is presented in Table IV. It can be seen that the $1s2s^2$ is strongly coupled with the $1s2p^2\,{}^2S$ state. The field effects on the energy levels $1s2s^2\,{}^2S_0$ and $1s2s2p\,{}^2P_{-1}$ may be found in Fig. 2, together with results for stable states. We have found that the magnetic field causes the energy of the autoionizing states to increase. We should mention that, in Ref. [7], the author found the similar magnetic-field effects on the resonance energies and widths for the ${}^1S^e(1)$ and ${}^1D^e(1)$ autoionizing states of H^- ion. In some cases, the field effects lead to the opening of new channels, which are forbidden in the case of no magnetic field. For the $1s2s^2\,{}^2S$ state, for example, in addition to the $1s^2+\epsilon s$ channel, a new channel associated with $1s2s\,{}^3S$ opens after the field strength reaches a strength of the order of 0.013 a.u. The magnetic field induces some additional complexities in the electronic properties of the negative ion. It is one of the decaying channels that with the unperturbed target $1s2s^2$ state decays into its own parent $1s2s\,{}^3S$ state while simultaneously emitting an electron. At first glance, the $1s2s^2$ state may be classified as a *potential shape resonance* for the $1s2s\,{}^3S+\epsilon s$ channel. But what mechanism produces such a penetrable barrier to trap the electron within the lifetime of the resonance state? In fact, the two-dimensional magnetic interaction proportional to $x_i^2+y_i^2$ confines the electron only in the x-y plane. The motion along the z axis remains free (in magnetic fields). Consider, for example, the $1s2s^2$ Landau excited state that lies above the $1s2s\,{}^3S_0$ threshold: there does not exist a three-dimensional penetrable barrier that can trap the electron within the resonance lifetime. Thus, for the channel $1s2s\,{}^3S+\epsilon s$, the $1s2s^2\,{}^2S_0$ is an autoionizing resonance induced by magnetic-field effects. On the other hand, the $1s^2+\epsilon s$ channel, in which the internal degrees of freedom of the target were changed is also open for this state. We have to distinguish then between two different mechanisms for the autoionizing process associated with the $1s^2+\epsilon s$ channel. Both the two-body repulsive interaction between electrons and the one-body diamagnetic interaction are dominant for the decay. We cannot, therefore, identify the state using the

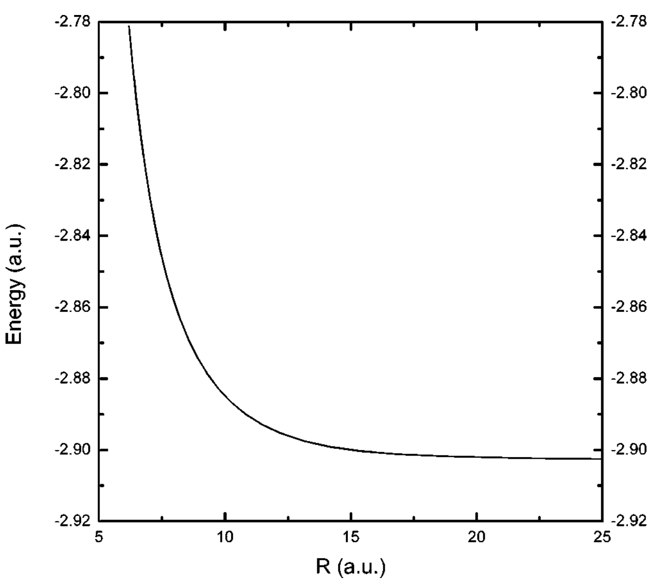

FIG. 8. Energy of the He^- *pseudo* $1s^22s$ state vs R at $\beta=0.01$ a.u. ($\beta=B/4.7011\times10^5$ T). The four angular components are used to describe the system. As one can see, no stationary point is found up to $R=25$ a.u. This indicated that at $\beta=0.01$ a.u. the He $1s^2$ state *cannot* attract an extra electron to form a stable He^- in the magnetic field.

TABLE IV. Energy convergence of the He^- ion $1s2s_0^2$ state at $\beta=0.01$ a.u. N is the number of terms included in the angular component. All the energies are in hartrees.

Angular component	N	$-\Delta E$
[(0,0)0,0]0	116	2.176 424 6
[(0,1)1,1]0	92	0.021 058 5
[(0,2)2,2]0	57	0.000 065 3
[(1,1)0,0]0	92	0.000 727 3
[(2,2)0,0]0	57	0.000 026 4
[(1,2)1,1]0	72	0.000 143 0
[(1,1)2,2]0	43	0.000 003 8
[(1,2)3,3]0	10	0.000 002 0
[(0,0)0,0]0[a]	97	0.000 228 0
[(0,1)1,1]0[a]	48	0.000 033 2
Total	684	2.198 712 2

[a]In these angular components, the spins of the first two electrons couple into a triplet.

standard notation without confusion. In other words, the different channels have to be individually emphasized for the $1s2s^2\,{}^2S$ state of He^- ion in magnetic fields.

For the $1s2s_0 2p_{-1}\,{}^2P_{-1}$, the new decay channel $1s2p_{-1}+\epsilon s$ will be open at a large enough field strength.

IV. CONCLUSION

In the present paper, the modified full core plus correlation and saddle-point techniques have been applied to calculations of the metastable and resonance states of He^- ion in a strong magnetic field. The nonlinear parameters of the basis sets were carefully optimized for each given field strength to yield reliable results. The energy range is limited below the He $1s2p\,{}^1P$ threshold. Given that compact, wave functions were used to describe the states of interest, it is not necessary to expand the wave function in terms of a very large number of basis functions. Correlation between the two active electrons is also accounted for in the present calculations.

The new phenomena induced by the magnetic fields were investigated. One of our interesting findings is that the $1s2p^2\,{}^4P_{-1}$ state, which is a shape resonance lying above the He $1s2p\,{}^3P$ threshold in the absence of the magnetic field, turns out to be a bound state (in the nonrelativistic approximation) when the magnetic field exceeds 0.002 a.u. (940 T). Other two bound states induced by field effects are also found. The effect of the field on autoionizing processes is another interesting result obtained. The autoionizing process is intricate given that the widths induced by the magnetic field are comparable to those in the field-free case.

Since spherical basis functions are used in this work, there remains room for improvement in the energy values. But we do not expect that a future refinement of calculations will change our main conclusions.

The negative helium ion is a quite weakly bound system compared with the H^- ion, and is very sensitive to the external field. We believe that the present calculations and conclusions will improve our understanding of the atomic systems in strong magnetic fields, especially for negative ions.

ACKNOWLEDGMENTS

This paper is supported by the National Natural Science Foundations of China under Grant Nos. 19734060 and 10004013. We are grateful to Professor S. P. Goldman for a critical reading of the manuscript.

[1] H. Ruder, G. Wunner, H. Herold, and F. Geyer, *Atoms in Strong Magnetic Fields* (Springer Verlag, Berlin, 1994), and references therein.
[2] K. M. Roussel and R. F. O'Connell, J. Phys. Chem. Solids **35**, 1429 (1974); J. Blinowski and T. Szwacka, Phys. Rev. B **49**, 10 231 (1994); D. M. Larsen, Phys. Rev. Lett. **42**, 742 (1979).
[3] J. Avron, I. Herbst, and B. Simon, Commun. Math. Phys. **79**, 525 (1981).
[4] O.-A. Al-Huajaj and P. Schmelcher, Phys. Rev. A **61**, 063413 (2000).
[5] V. G. Bezchastnov, P. Schmelcher, and L. S. Cederbaum, Phys. Rev. A **61**, 052512 (2000).
[6] J. Avron, I. Herbst, and B. Simon, Phys. Rev. Lett. **39**, 1068 (1977).
[7] Y. K. Ho, Phys. Rev. A **56**, 3630 (1997); J. Phys. B **31**, 1191 (1998).
[8] S. Jordan, P. Schmelcher, W. Becken, and W. Schweizer, Astron. Astrophys. **336**, L33 (1998).
[9] W. Becken and P. Schmelcher, J. Phys. B **33**, 545 (2000).
[10] K. T. Chung, Phys. Rev. A **44**, 5421 (1991).
[11] K. T. Chung, Phys. Rev. A **23**, 2957 (1981); **24**, 1350 (1981).
[12] Y. K. Ho and Z.-C. Yan, Phys. Rev. A **59**, R2559 (1999).
[13] A. V. Bunge and C. F. Bunge, Phys. Rev. A **30**, 2179 (1984); P. Kristensen, U. V. Pedersen, V. V. Petrunin, T. Andersen, and K. T. Chung, *ibid.* **55**, 978 (1997).
[14] K. T. Chung, Phys. Rev. A **23**, 1079 (1981).
[15] S. J. Buckman and C. W. Clark, Rev. Mod. Phys. **66**, 539 (1994), and references therein.
[16] M. Bylicki, J. Phys. B **30**, 189 (1997).
[17] G. W. F. Drake and Z.-C. Yan, Phys. Rev. A **46**, 2378 (1992).
[18] A. Scrinzi, Phys. Rev. A **58**, 3879 (1998).
[19] K. T. Chung and J. C. Chang, Phys. Rev. A **61**, 030701 (2000).
[20] K. T. Chung, Phys. Rev. A **58**, 2777 (1998).